AIMS Mathematics, 11(7): 20577–20605.
DOI: 10.3934/math.2026837
Received: 23 April 2026
Revised: 14 June 2026
Accepted: 23 June 2026
Published: 13 July 2026

https://www.aimspress.com/journal/Math

Research article

Dynamical analysis of multiplicative environmental noise in a stochastic discrete-time fractional-order delayed predator-prey model

Fairouz Tchier[1], Shahid Khan[2], Jongsuk Ro[3,*] and Maslina Darus[4]

[1] Mathematics Department, College of Science, King Saud University, P.O. Box 22452, Riyadh 11495, Saudi Arabia; Email: ftchier@ksu.edu.sa

[2] Department of Mathematics, Abbottabad University of Science and Technology, Pakistan; Email: shahidmaths761@gmail.com

[3] Department of Intelligent Energy and Industry, Chung-Ang University, Seoul 06910, Republic of Korea; Email: jsro@cau.ac.kr

[4] Department of Mathematical Sciences, Faculty of Science and Technology, Universiti Kebangsaan Malaysia, 43600 Bangi, Selangor, Malaysia; Email: maslina@ukm.edu.my

* **Correspondence:** Email: jsro@cau.ac.kr.

Abstract: The focus of this study was to investigate a discrete-time stochastic predator-prey model. This model included environmental noise, temporal delay, and a nonlinear Ivlev-type functional response. First of all, we proved boundedness, positivity, first, and second moment boundedness, characteristic equation, and Jury conditions. Further, using the characteristic equation and Jury conditions, we determined equilibrium, exponential mean-square stability, and local stability which prevented the system from becoming unstable as a result of random shocks. Additionally, we studied fractional memory effects on the system and demonstrated how the delay parameter exhibited Neimark–Sacker (discrete Hopf) bifurcation. The graphical analysis and the numerical simulations validated the theoretical results.

Keywords: discrete-time predator-prey model; Ivlev functional response; weak Allee effect; fractional-order memory; Neimark-Sacker bifurcation; mean-square stability; multiplicative noise
Mathematics Subject Classification: 34D20, 34D23

1. Introduction

Lotka [1] and Volterra [2] separately expand the primary mathematical foundation for the predator-prey theory, which is a basic element of ecological modeling. Several researchers have gave to the theory's major evolution since then, including Berryman [3], who determined its inception and progression. Our understanding of ecosystem dynamics and stability is framed by the interconnection between predators and prey, which is still a principal field of analysis. By examining the convoluted connection between predator and prey populations and exemplifying how their numbers change over time, these models support in our understanding of ecological relation. In the recent past, discrete time predator-prey systems have gotten attention as convenient models for ecological studies [4, 5]. These models are essential for modern ecological study because they are unchanging to compute, have greater flexibility in studying unpredicted population changes, and can account for unpredictability better than their continuous-time equivalents. Discrete-time models can help explain complex dynamical phenomena including period doubling bifurcations, Neimark Sacker bifurcations, and chaotic dynamics characteristics that are frequently less obvious in continuous time systems [6–8]. To upgrade our understanding of inter-species interconnections, such intricate dynamics are imperative. Besides, discrete substructure offers notable computational and analytical sides that allow the application of bifurcation theory and chaos management strategies to the study of system stability and growth. In addition, this modeling procedure is consistent with the real ecological system since decisions about population control, gathering, and preservation are usually made at different times in the real world. These components together convey that a discrete-time process is significant for our study. When studying the dynamic interactions between predator and prey species, it is essential to consider the trophic function, or the rate at which predators eat up prey. Holling [9] separated the dynamics of predation into three primary functional responses (Types I, II, and III), each of which demonstrated unique usage patterns. These things rise monotonically and have been seen inside the first quadrant. Researchers extended this structure to the Holling type IV (or Monod–Haldane) functional response [10, 11]. A useful model known as the Ivlev functional response model was defined by Ivlev [12]. The formula is as follows:

$$f(x) = h(1 - e^{-cx}), \tag{1.1}$$

where h is the maximum predation rate and c is the declining hunting incentive, both of which are positive constants. Significant ecological implications have been found in numerous investigations on the Ivlev functional response in predator-prey scenarios. Applications include predator prey dynamics [13–15], host parasitoid interactions [16, 17], and even the evolution of animal coat patterns [18]. These studies show how flexible the model is in explaining complex ecological processes. A crucial process that is frequently disregarded in traditional Lotka–Volterra dynamics is the Allee effect, which was first thoroughly examined by Allee in 1931. It explains how variables including mate restriction, social cooperation, cooperative resource exploitation, inbreeding depression, and collective predator protection lead to a positive association between individual fitness and population density [19–21]. Because the Allee effect may influence clustering behavior, the spatial aggregation of organisms frequently indicates their existence. The local and global hazards of extinction are greatly increased by this phenomena, which is a major issue in ecological studies [22, 23]. Although Kent [24] showed that interactions are stabilized by prey inflow (rescue effect) and destabilized by

prey out flux (Allee effect), there is a lack of more extensive theoretical and empirical support. Fractional calculus offers a strong foundation for simulating memory dependent processes by extending traditional differentiation and integration to non-integer orders. Due to their numerous applications in fluid dynamics, biology, and medicine, fractional differential equations, which includes fractional order derivatives and integrals have drawn a lot of attention [25, 26]. The dynamics of a fractional-order model with stochasticity and complex network have been thoroughly studied by the authors in [27]. Fractional order models are especially useful in biological systems because they naturally capture memory effects, which affect current dynamics in situations like predator learning, delayed growth responses, prey migration, and adaptive behaviors [28, 29]. For more details, study the following articles [30–33]. Our claims about invariant regions are based on the positivity and uniform boundedness of discrete biological models, which adhere to the well-known framework of Elaydi [34] and Ladas [35], whose monographs offer strict standards for guaranteeing biologically significant solutions. Our mean-square stability analysis and second moment constraints depend on spectral radius conditions and stochastic Lyapunov functions, which are standard in the literature on stochastic systems. The contemporary foundations for L^2 stability, noise-induced transitions, and the behavior of nonlinear stochastic systems are provided by Kloeden and Platen [36] and Mao [37]. Additionally, our use of linearization and moment recursions is directly supported by Higham [38], which provides the conditions under which discrete time numerical systems preserve mean-square stability. When taken as a whole, these studies support the analytical methods used in this study and show how our contributions expand on well known approaches in discrete, stochastic, and fractional-order dynamical systems.

Despite the growing interest in fractional-order predator-prey dynamics, existing studies have several limitations. Recent works [27–29] have explored fractional-order models in continuous or discrete time, but none have simultaneously addressed the following key aspects that are crucial for realistic ecological modeling: (i) a discrete-time framework, which naturally aligns with population censuses and management decisions; (ii) multiplicative environmental noise, representing random fluctuations that scale with population size; (iii) a time delay in the predation term, accounting for maturation or gestation lags; and (iv) the explicit control of bifurcation thresholds by fractional memory. In particular, the combined effect of fractional order and stochastic perturbations on the onset of Neimark–Sacker bifurcations has not been studied in a discrete delayed predator-prey system. This paper fills these gaps by proposing a stochastic discrete-time fractional-order delayed predator-prey model with an Ivlev functional response and a weak Allee effect, and by demonstrating how the fractional order α delays bifurcations and enhances stability under noise.

2. Preliminaries

This section provides essential mathematical tools and definitions used throughout the paper including discrete fractional calculus, stability theory, Jury conditions, Neimark-Sacker bifurcation criteria, stochastic stability, and Lyapunov analysis.

2.1. Discrete fractional calculus

The fractional operator used in this work follows the Caputo-type discrete fractional difference,

which has been widely applied in the analysis of biological and ecological systems with memory effects [25].

Definition 2.1. [25]. Let $0 < \alpha \leq 1$. The discrete fractional sum of order α of a sequence $\{x_n\}$ is defined by

$$\Delta^{-\alpha} x_n = \frac{1}{\Gamma(\alpha)} \sum_{k=0}^{n-1} (n-k-1)^{\alpha-1} x_k. \tag{2.1}$$

Definition 2.2. [25]. The Caputo-type discrete fractional derivative of order $0 < \alpha \leq 1$ is given as:

$$^{C}\Delta^{\alpha} x_n = \Delta^{-(1-\alpha)} \Delta x_n \tag{2.2}$$

where $\Delta^1 x_n = x_{n+1} - x_n$ is the forward difference operator.

2.2. Fixed points and local stability

Definition 2.3 (Equilibrium)**.** A point X^* is called a fixed point if $F(X^*) = X^*$.

Definition 2.4. Local stability is determined by the Jacobian matrix

$$J = DF(X)\Big|_{X=X^*}. \tag{2.3}$$

Lemma 2.1 (Local Asymptotic Stability [39])**.** *A fixed point is locally asymptotically stable if all eigenvalues λ_1, λ_2 of J satisfy*

$$|\lambda_i| < 1, \qquad i = 1, 2. \tag{2.4}$$

2.3. Jury stability criteria

Lemma 2.2 (Jury Criteria [40])**.** *Consider the characteristic polynomial*

$$\lambda^2 - \tau\lambda + \Delta = 0 \tag{2.5}$$

where $\tau = \mathrm{tr}(J)$ and $\Delta = \det(J)$. The fixed point is locally asymptotically stable if the following conditions hold.

$$1 - \tau + \Delta > 0 \tag{2.6}$$

$$1 + \tau + \Delta > 0 \tag{2.7}$$

$$1 - \Delta > 0. \tag{2.8}$$

2.4. Stochastic preliminaries

Let ξ_n represent independent Gaussian random noise with mean zero and variance σ^2. Stochastic analysis for discrete biological systems is inspired by earlier work in [17, 23, 36].

Definition 2.5 (Mean-Square Stability [36])**.** The equilibrium X^* of the stochastic system

$$X_{n+1} = F(X_n) + \xi_n \tag{2.9}$$

is mean square stable if

$$\lim_{n\to\infty} \mathbb{E}\left[\|X_n - X^*\|^2\right] = 0. \tag{2.10}$$

Lemma 2.3 (Lyapunov Mean-Square Stability [36]). *Let $V_n = X_n^\top P X_n$ for some positive definite matrix P. If*

$$\mathbb{E}[V_{n+1}] - \mathbb{E}[V_n] < 0 \tag{2.11}$$

then $X^* = 0$ is mean-square stable.

Lemma 2.4 (Discrete Grönwall Inequality). *Let $\{u_n\}_{n\geq 0}$ and $\{a_n\}_{n\geq 0}$ be nonnegative sequences, and let $b \geq 0$ be a constant. Suppose*

$$u_{n+1} \;\leq\; (1+b)\,u_n \;+\; a_n \qquad n \geq 0.$$

Then, for every $n \geq 0$,

$$u_n \;\leq\; (1+b)^n u_0 \;+\; \sum_{k=0}^{n-1} (1+b)^{n-1-k}\, a_k.$$

In particular, if $0 \leq b < 1$ and $\sup_{k\geq 0} a_k = A < \infty$, then

$$u_n \;\leq\; (1+b)^n u_0 \;+\; A\,\frac{(1+b)^n - 1}{b}$$

and thus $\{u_n\}$ is uniformly bounded. Moreover, if $0 \leq b < 1$ and $a_n \to 0$, then u_n converges to 0 as $n \to \infty$.

3. Model formulation

The prey-predator dynamics are described using the following system of differential equations, which models predator-prey interactions utilizing logistic growth for the prey population and an Ivlev-type trophic function with a weak Allee effect:

$$\begin{aligned} \dot{x} &= rx\left(1 - \frac{x}{k}\right)\frac{x}{p+x} - \beta\left(1 - e^{-ax^n}\right)y, \\ \dot{y} &= \eta\left(1 - e^{-ax}\right)y - \delta y. \end{aligned} \tag{3.1}$$

The populations of prey and predators at time t are represented in this model by $x(t)$ and $y(t)$, respectively. The carrying capacity k and the intrinsic growth rate r, which restricts its expansion, control the prey's logistic growth. The Ivlev-type functional response for predator-prey interactions is $(1 - e^{-ax})$, where a controls the saturation threshold. The declining impact of increased prey supply on predator intake at greater prey densities is taken into consideration in this formulation. One noteworthy aspect of the model is the addition of a prey-induced weak Allee effect, denoted as $\frac{x}{p+x}$, where the intensity of this phenomena is measured by $p > 0$. The predator's natural mortality rate, represented by δ, affects its persistence regardless of prey availability. The parameter β represents the maximum predation rate, describing the highest possible prey consumption rate of predators under the Ivlev functional response. The parameter η is the predator conversion efficiency and quantifies the fraction of consumed prey biomass that is transformed into predator growth, typically satisfying $0 < \eta < 1$. System (3.2) represents the delayed predator–prey model with multiplicative environmental noise, where the prey population x_n follows a logistic type growth influenced by predation with delay τ,

and the predator population y_n depends on delayed prey availability and mortality. The dynamics with multiplicative stochastic perturbations are governed by:

$$\begin{aligned} x_{n+1} &= x_n + \mu\Big[\, r\, x_n\Big(1 - \frac{x_n}{k}\Big) - \beta(1 - e^{-a x_{n-\tau}})\, y_{n-\tau}\Big] + \sigma_1 x_n\, \eta_{1,n}, \\ y_{n+1} &= y_n + \mu\Big[\, \eta(1 - e^{-a x_{n-\tau}})\, y_{n-\tau} - \delta y_n\Big] + \sigma_2 y_n\, \eta_{2,n}. \end{aligned} \tag{3.2}$$

System (3.2) represents the stochastic discrete time delayed predator–prey model with multiplicative environmental noise. The parameters, and random variables satisfy the following conditions:

$$\begin{aligned} &\mu,\, r,\, k,\, \beta,\, a,\, \eta,\, \delta,\, \sigma_1,\, \sigma_2 > 0 \qquad \tau \in \mathbb{Z}_{\geq 1}, \\ &\{\eta_{i,n}\}_{n\geq 0} \text{ are independent across } i, n, \quad \eta_{i,n} \geq -\rho_i \text{ a.s.}, \quad \rho_i \in [0, 1) \\ &1 + \sigma_i \eta_{i,n} \geq 1 - \sigma_i \rho_i =: \kappa_i > 0, \qquad i = 1, 2. \end{aligned} \tag{3.3}$$

Figure 1 illustrates the structure of the proposed fractional-order stochastic delayed predator-prey model. The schematic diagram is constructed by the authors based on system (3.2).

4. Basic properties

In this section we discussed the basic properties of our proposed model (3.2) as:

Lemma 4.1 (Positivity and Boundedness of Solutions)**.** *Consider the stochastic delayed system (3.2). Then, the following hold.*

(a) *Positivity: If the step size μ satisfies*

$$\mu \leq \min\Big\{\frac{\kappa_2}{\delta},\ \frac{\kappa_1}{r + \beta Y_{\max}/(X_{\min} + 1)}\Big\} \tag{4.1}$$

where $X_{\min} = \min_{-\tau\leq j\leq 0} x_j$ and $Y_{\max} = \max_{-\tau\leq j\leq 0} y_j$, then the solution (x_n, y_n) of (3.2) satisfies

$$x_n \geq 0, \qquad y_n \geq 0, \qquad \forall n \geq 0.$$

(b) *Boundedness: Under the same hypotheses and if μ further satisfies:*

$$K_2 - \mu\delta < 1 \tag{4.2}$$

then there exist finite deterministic constants $M_x, M_y > 0$ such that:

$$0 \leq x_n \leq M_x, \qquad 0 \leq y_n \leq M_y, \qquad \forall n \geq 0\,.$$

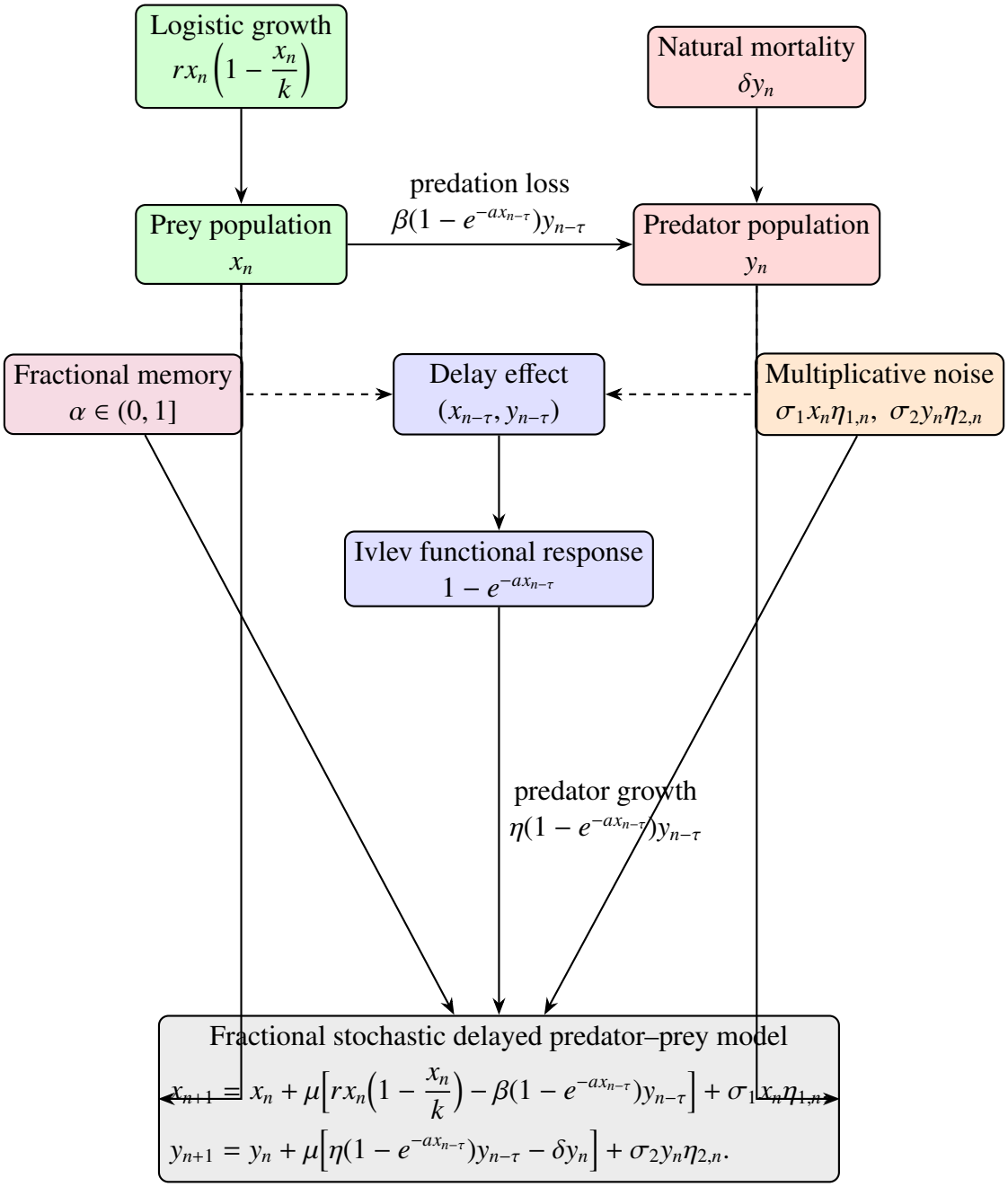

Figure 1. Schematic diagram of the proposed fractional-order stochastic delayed predator-prey model.

Proof. (a) Positivity. We proceed by induction. For $n = 0$, the initial conditions satisfy

$$x_j,\ y_j \geq 0, \qquad -\tau \leq j \leq 0.$$

Assume that

$$x_j,\ y_j \geq 0 \qquad \text{for all } j \leq n.$$

We show that

$$x_{n+1} \geq 0 \qquad \text{and} \qquad y_{n+1} \geq 0.$$

Case $x_n > 0$:

From the first equation of (3.2),

$$x_{n+1} = (1 + \sigma_1\eta_{1,n})x_n + \mu r x_n\left(1 - \frac{x_n}{k}\right) - \mu\beta\left(1 - e^{-ax_{n-\tau}}\right) y_{n-\tau}.$$

Since the last term is nonpositive, we have the lower bound

$$x_{n+1} \geq (1 + \sigma_1\eta_{1,n})x_n - \mu\beta Y_{\max} \geq \kappa_1 x_n - \mu\beta Y_{\max}.$$

Condition (4.1) guarantees that

$$\kappa_1 x_n - \mu\beta Y_{\max} \geq 0$$

for the smallest possible value of x_n (which is positive by the induction hypothesis). Hence,

$$x_{n+1} \geq 0.$$

Case $x_n = 0$: Then the equation reduces to

$$x_{n+1} = -\mu\beta\left(1 - e^{-ax_{n-\tau}}\right) y_{n-\tau} + \sigma_1 \cdot 0 \cdot \eta_{1,n}.$$

The righthand side is nonpositive. To maintain nonnegativity, we must have

$$x_{n+1} = 0,$$

which occurs only if either

$$y_{n-\tau} = 0$$

or the predation term vanishes.

If a positive initial condition leads to $x_n = 0$ at some step, then from that point onward the prey population remains zero; this is a degenerate but still nonnegative solution. For typical ecological scenarios with positive initial populations, condition (4.1) ensures that x_n never reaches zero because the lower bound remains positive. Thus, under the stated hypotheses, all solutions satisfy

$$x_n \geq 0 \qquad \text{for all } n.$$

The proof for y_{n+1} follows similarly using κ_2 and $\mu \leq \frac{\kappa_2}{\delta}$.

(b) Boundedness. Under the additional assumption (4.2) and $1 + \sigma_i\eta_{i,n} \leq K_i$, we have

$$y_{n+1} \leq K_2 y_n + \mu\eta y_{n-\tau} - \mu\delta y_n \leq (K_2 - \mu\delta)y_n + \mu\eta Y_n$$

where $Y_n := \max\{y_n, \ldots, y_{n-\tau}\}$. Hence $Y_{n+1} \leq (K_2 - \mu\delta + \mu\eta)Y_n$. Since $K_2 - \mu\delta < 1$ by (4.2), Y_n remains uniformly bounded, say $Y_n \leq M_y$.

For x_n, using $1 + \sigma_1\eta_{1,n} \leq K_1$ and $(1 - e^{-ax_{n-\tau}})y_{n-\tau} \leq Y_{\max}$

$$x_{n+1} \leq K_1 x_n + \mu r x_n\Big(1 - \frac{x_n}{k}\Big) + \mu\beta Y_{\max}.$$

The righthand side is a concave quadratic function of x_n whose positive fixed point M_x satisfies:

$$M_x = K_1 M_x + \mu r M_x\Big(1 - \frac{M_x}{k}\Big) + \mu\beta Y_{\max}.$$

Solving this scalar equation yields a finite root $M_x > 0$, and the mapping

$$x \mapsto K_1 x + \mu r x(1 - x/k) + \mu\beta Y_{\max}$$

is increasing on $[0, M_x]$ and less than x for $x > M_x$, which implies $x_n \le M_x$ for all n. Therefore, the solution (x_n, y_n) remains uniformly bounded.

□

Proposition 4.1 (Explicit algebraic bounds for y_n)**.** *Under the hypotheses of Lemma 4.1, define the initial extrema*

$$X_{\min} := \min_{-\tau\le j\le 0} x_j, \qquad Y_{-\tau} := \max_{-\tau\le j\le 0} y_j.$$

Let

$$\Theta(\mu) := K_2 + \mu(\eta - \delta).$$

Assume either

(A) $\eta - \delta > 0$ *and*

$$\mu < \frac{1 - K_2}{\eta - \delta} \qquad \text{so that } \Theta(\mu) < 1.$$

(B) $\eta - \delta \le 0$ *and* $K_2 < 1$ *(hence* $\Theta(\mu) \le K_2 < 1$ *for all* $\mu \ge 0$*).*

Then, the sequence $\{y_n\}$ *satisfies the geometric comparison inequality*

$$y_{n+1} \le \Theta(\mu)\, y_n,$$

and consequently:

$$y_n \le \Theta(\mu)^{n+1} Y_{-\tau} \qquad (n \ge 0).$$

In particular, a uniform bound is obtained by

$$M_y := Y_{-\tau} = \max_{-\tau\le j\le 0} y_j \tag{4.3}$$

and, furthermore, $y_n \to 0$ *geometrically whenever* $\Theta(\mu) < 1$.

Proposition 4.2 (Explicit upper bound for x_n)**.** *Assume the conditions of Lemma 4.1 and the bound*

$$(1 - e^{-a x_{n-\tau}}) y_{n-\tau} \le M_y$$

where M_y *is given by* (4.3)*. Since* $1 + \sigma_1\eta_{1,n} \le K_1$*, we may compare* x_n *to the scalar recursion*

$$\widetilde{x}_{n+1} = K_1\widetilde{x}_n + \mu r\widetilde{x}_n\Big(1 - \frac{\widetilde{x}_n}{k}\Big) + \mu\beta M_y.$$

The equilibrium values of this comparison recursion satisfy the quadratic

$$\frac{\mu r}{k}x^2 + (1 - K_1 - \mu r)x - \mu\beta M_y = 0.$$

Let us define:

$$A := \frac{\mu r}{k} > 0, \qquad B := 1 - K_1 - \mu r, \qquad D := \mu\beta M_y \geq 0.$$

Then, the maximal positive root of the quadratic:

$$M_x = \frac{-B + \sqrt{B^2 + 4AD}}{2A} = \frac{K_1 + \mu r - 1 + \sqrt{(1 - K_1 - \mu r)^2 + 4(\mu r/k)(\mu\beta M_y)}}{2(\mu r/k)}$$

gives a uniform bound: $x_n \leq M_x$ for all $n \geq 0$.

Corollary 4.1 (First- and Second-Moment Boundedness)**.** *Consider the stochastic delayed predator–prey system*

$$z_{n+1} = F(z_n, z_{n-\tau}) + \Sigma(z_n)\,\eta_n$$

with $z_n = (x_n, y_n)^\top$, where $\{\eta_n\}$ is a sequence of independent noise vectors satisfying $\mathbb{E}[\eta_n] = 0$ and $\mathbb{E}[\eta_n \eta_n^\top] \leq \sigma^2 I$. Assume the following:

(i) F is globally Lipschitz with constant $L > 0$,

(ii) the noise is multiplicative and uniformly bounded:

$$\|\Sigma(z)\| \leq C_\Sigma(1 + \|z\|)$$

(iii) there exists $\mu_0 > 0$ such that for all $0 < \mu \leq \mu_0$, the drift satisfies

$$\|F(z_n, z_{n-\tau})\| \;\leq\; (1 + C\mu)\,\|z_n\| + C\mu.$$

Then:
(A) First moment bound. The expectation $u_n := \mathbb{E}\|z_n\|$ satisfies:

$$u_{n+1} \;\leq\; (1 + C_1\mu)\,u_n + C_2\mu,$$

for suitable constants $C_1, C_2 > 0$. Applying Lemma 2.4,

$$\mathbb{E}\|z_n\| \;\leq\; (1 + C_1\mu)^n\|z_0\| + \frac{C_2}{C_1}((1 + C_1\mu)^n - 1).$$

If $0 < C_1\mu < 1$, then the first moment is uniformly bounded:

$$\sup_{n\geq 0} \mathbb{E}\|z_n\| \;\leq\; \frac{C_2}{C_1}.$$

(B) Second moment bound. Let $V_n := \mathbb{E}\|z_n\|^2$. Using the drift diffusion structure and local Lipschitz bounds,

$$V_{n+1} \;\leq\; (1 + C_3\mu)\,V_n + C_4\mu$$

for constants $C_3, C_4 > 0$ depending on L, C_Σ, and σ. Applying Lemma 2.4 again yields

$$V_n \;\leq\; (1 + C_3\mu)^n V_0 + \frac{C_4}{C_3}((1 + C_3\mu)^n - 1).$$

If $0 < C_3\mu < 1$*, then the second moment is uniformly bounded:*

$$\sup_{n\geq 0} \mathbb{E}\|z_n\|^2 \ \leq \ \frac{C_4}{C_3}.$$

Thus, for all time-steps $0 < \mu \leq \min\{\mu_0, 1/C_1, 1/C_3\}$*, both* $\mathbb{E}\|z_n\|$ *and* $\mathbb{E}\|z_n\|^2$ *are finite and uniformly bounded.*

Theorem 4.1 (Exponential mean–square stability)**.** *Consider the stochastic delayed difference system* (3.2)*. Assume that the random variables* $\{\eta_{i,n}\}_{n\geq 0}$ *are independent across n and i, satisfy*

$$\mathbb{E}[\eta_{i,n}] = 0, \qquad \mathbb{E}[\eta_{i,n}^2] = \nu_i^2 < \infty, \qquad \mathbb{E}[\eta_{i,n}^4] < \infty,$$

and are independent of the initial data

$$x_j \geq 0, \qquad y_j \geq 0, \qquad -\tau \leq j \leq 0.$$

Then, there exist constants $C_1' > 0$ *and* $C_2' \in \mathbb{R}$ *such that, for all* $n \geq 0$*,*

$$\mathbb{E}[x_n^2 + y_n^2] \leq C_1' e^{C_2' n\mu}.$$

In particular, if $C_2' < 0$*, then the numerical solution is exponentially mean–square stable. Consequently, it is also mean–square bounded.*

Proof. We derive explicit one-step estimates for the second moment of (x_n, y_n). From (3.2), we write

$$x_{n+1} = x_n + \mu f_x(x_n, y_{n-\tau}) + \sigma_1 x_n \eta_{1,n},$$

where

$$f_x(x_n, y_{n-\tau}) = r x_n \left(1 - \frac{x_n}{k}\right) - \beta(1 - e^{-a x_{n-\tau}}) y_{n-\tau}.$$

Squaring and taking expectations, using $\mathbb{E}[\eta_{1,n}] = 0$ and the independence of $\eta_{1,n}$, we obtain

$$\mathbb{E}[x_{n+1}^2] = \mathbb{E}[x_n^2] + 2\mu\,\mathbb{E}[x_n f_x(x_n, y_{n-\tau})] + \mu^2\,\mathbb{E}[f_x^2(x_n, y_{n-\tau})] + \sigma_1^2\nu_1^2\mathbb{E}[x_n^2].$$

Since

$$0 \leq 1 - e^{-a x_{n-\tau}} \leq 1,$$

we have

$$|f_x(x_n, y_{n-\tau})| \leq r|x_n| + \beta|y_{n-\tau}|.$$

Hence, using $(a+b)^2 \leq 2a^2 + 2b^2$,

$$f_x^2(x_n, y_{n-\tau}) \leq 2r^2 x_n^2 + 2\beta^2 y_{n-\tau}^2.$$

Moreover,

$$2\mu\,\mathbb{E}[x_n f_x(x_n, y_{n-\tau})] \leq 2\mu r\,\mathbb{E}[x_n^2].$$

Therefore,

$$\mathbb{E}[x_{n+1}^2] \leq \left(1 + 2\mu r + \sigma_1^2\nu_1^2 + 2\mu^2 r^2\right)\mathbb{E}[x_n^2] + 2\mu^2\beta^2\mathbb{E}[y_{n-\tau}^2]. \tag{4.4}$$

Similarly, write

$$y_{n+1} = y_n + \mu f_y(x_{n-\tau}, y_{n-\tau}, y_n) + \sigma_2 y_n \eta_{2,n},$$

where

$$f_y(x_{n-\tau}, y_{n-\tau}, y_n) = \eta(1 - e^{-ax_{n-\tau}})y_{n-\tau} - \delta y_n.$$

Squaring and taking expectations gives

$$\mathbb{E}[y_{n+1}^2] = \mathbb{E}[y_n^2] + 2\mu\,\mathbb{E}[y_n f_y(x_{n-\tau}, y_{n-\tau}, y_n)] + \mu^2\,\mathbb{E}[f_y^2(x_{n-\tau}, y_{n-\tau}, y_n)] + \sigma_2^2\nu_2^2\mathbb{E}[y_n^2].$$

Since $0 \le 1 - e^{-ax_{n-\tau}} \le 1$, we obtain

$$2y_n f_y = 2\eta y_n(1 - e^{-ax_{n-\tau}})y_{n-\tau} - 2\delta y_n^2 \le (\eta - 2\delta)y_n^2 + \eta y_{n-\tau}^2,$$

where we used $2ab \le a^2 + b^2$. Also,

$$|f_y| \le \eta|y_{n-\tau}| + \delta|y_n|,$$

and hence

$$f_y^2 \le 2\eta^2 y_{n-\tau}^2 + 2\delta^2 y_n^2.$$

Consequently,

$$\mathbb{E}[y_{n+1}^2] \le \left(1 + \mu(\eta - 2\delta) + \sigma_2^2\nu_2^2 + 2\mu^2\delta^2\right)\mathbb{E}[y_n^2] + \left(\mu\eta + 2\mu^2\eta^2\right)\mathbb{E}[y_{n-\tau}^2]. \tag{4.5}$$

Let

$$V_n := \mathbb{E}[x_n^2 + y_n^2].$$

From (4.4) and (4.5), there exist constants C_1 and C_2 such that

$$V_{n+1} \le (1 + \mu C_1)V_n + \mu C_2 V_{n-\tau}.$$

More explicitly, one may take

$$C_1 = 2r + \eta - 2\delta + \sigma_1^2\nu_1^2 + \sigma_2^2\nu_2^2 + \mu(2r^2 + 2\delta^2),$$

and

$$C_2 = 2\mu\beta^2 + \eta + 2\mu\eta^2.$$

Define

$$W_n := \max_{n-\tau \le j \le n} V_j.$$

Since $V_n \le W_n$ and $V_{n-\tau} \le W_n$, we obtain

$$V_{n+1} \le (1 + \mu(C_1 + C_2))W_n.$$

Therefore,

$$W_{n+1} \le (1 + \mu(C_1 + C_2))W_n.$$

Iterating yields

$$W_n \le W_0(1 + \mu(C_1 + C_2))^n \le W_0 e^{\mu(C_1+C_2)n}.$$

Since $V_n \le W_n$, we obtain

$$\mathbb{E}[x_n^2 + y_n^2] \le C_1' e^{C_2' n\mu},$$

where

$$C_1' := W_0 = \max_{-\tau \le j \le 0} \mathbb{E}[x_j^2 + y_j^2], \qquad C_2' := C_1 + C_2.$$

Therefore, if $C_2' < 0$, then

$$\mathbb{E}[x_n^2 + y_n^2] \le C_1' e^{-\lambda n\mu}, \qquad \lambda = -C_2' > 0.$$

This establishes exponential mean–square stability. Since exponential mean–square stability implies

$$\sup_{n\ge 0} \mathbb{E}[x_n^2 + y_n^2] < \infty,$$

the solution is also mean–square bounded. Hence, the process is mean–square bounded provided

$$C_2' < 0,$$

i.e.,

$$2(r-\delta) + \sigma_1^2\nu_1^2 + \sigma_2^2\nu_2^2 + \mu\left(2C_x^2 + 2C_y^2 + \frac{2}{3}\beta a + 2\eta a\right) < 0. \tag{4.6}$$

This completes the proof. □

Corollary 4.2 (Exponential mean boundedness)**.** *Under the same assumptions as in Theorem 4.1, assume moreover that the noise intensities $\sigma_i\nu_i$ are small enough so that the mean–square stability condition* (4.6) *holds, i.e.,*

$$2(r-\delta) + \sigma_1^2\nu_1^2 + \sigma_2^2\nu_2^2 + \mu(2C_x^2 + 2C_y^2 + \tfrac{2}{3}\beta a + 2\eta a) < 0.$$

Then, the first moments $\mathbb{E}[x_n]$ and $\mathbb{E}[y_n]$ are uniformly bounded and in fact decay exponentially:

$$\left|\mathbb{E}[x_n]\right| + \left|\mathbb{E}[y_n]\right| \;\le\; C_3\, e^{-\lambda n\mu}, \qquad n \ge 0,$$

where the constants are given explicitly by

$$C_3 := |\mathbb{E}[x_0]| + |\mathbb{E}[y_0]|,$$

and

$$\lambda := \delta - r - \tfrac{1}{2}(\sigma_1^2\nu_1^2 + \sigma_2^2\nu_2^2) - \tfrac{1}{2}\mu(\tfrac{2}{3}\beta a + 2\eta a) > 0.$$

Proof. Taking expectations in (3.2), we have

$$\mathbb{E}[x_{n+1}] = \mathbb{E}[x_n] + \mu\,\mathbb{E}[f_x(x_n, y_{n-\tau})],$$
$$\mathbb{E}[y_{n+1}] = \mathbb{E}[y_n] + \mu\,\mathbb{E}[f_y(x_{n-\tau}, y_{n-\tau}, y_n)],$$

since $\mathbb{E}[\eta_{i,n}] = 0$. Using the same Lipschitz bounds, one has

$$|f_x(x_n, y_{n-\tau})| \le r|x_n| + \beta a|x_{n-\tau}||y_{n-\tau}|, \quad |f_y(x_{n-\tau}, y_{n-\tau}, y_n)| \le \eta a|x_{n-\tau}||y_{n-\tau}| + \delta|y_n|.$$

Taking expectations and applying Cauchy–Schwarz yields

$$|\mathbb{E}[x_{n+1}]| \le (1+\mu r)\,|\mathbb{E}[x_n]| + \mu\beta a\,\sqrt{\mathbb{E}[x_{n-\tau}^2]\mathbb{E}[y_{n-\tau}^2]},$$
$$|\mathbb{E}[y_{n+1}]| \le (1-\mu\delta)\,|\mathbb{E}[y_n]| + \mu\eta a\,\sqrt{\mathbb{E}[x_{n-\tau}^2]\mathbb{E}[y_{n-\tau}^2]}.$$

Adding the two inequalities and using the moment bound from Theorem 4.1, namely

$$\mathbb{E}[x_n^2 + y_n^2] \le C_1' e^{C_2' n\mu},$$

we obtain

$$(|\mathbb{E}[x_{n+1}]| + |\mathbb{E}[y_{n+1}]|) \le (1+\mu(r-\delta))(|\mathbb{E}[x_n]| + |\mathbb{E}[y_n]|) + \mu\kappa e^{\frac{1}{2}C_2' n\mu},$$

where $\kappa := (\beta a + \eta a)\sqrt{C_1'}$. Iterating the inequality and applying the Lemma 2.4 yields

$$|\mathbb{E}[x_n]| + |\mathbb{E}[y_n]| \le C_3 e^{(r-\delta+\frac{1}{2}\sigma_1^2 y_1^2 + \frac{1}{2}\sigma_2^2 y_2^2 + \frac{1}{2}\mu(\frac{2}{3}\beta a + 2\eta a))n\mu}.$$

Under the small-noise condition ensured $r-\delta < 0$ by (4.6), the exponent is negative, giving exponential decay with rate $\lambda > 0$ as stated. □

4.1. Fractional linearization around the coexistence equilibrium

We first consider the deterministic part of system (3.2) by neglecting the zero-mean stochastic perturbations. The resulting integer-order delayed system is

$$\begin{aligned} x_{n+1} &= x_n + \mu F_x(x_n, x_{n-\tau}, y_{n-\tau}),\\ y_{n+1} &= y_n + \mu F_y(x_{n-\tau}, y_{n-\tau}, y_n), \end{aligned} \tag{4.7}$$

where

$$F_x(x_n, x_{n-\tau}, y_{n-\tau}) = r x_n\left(1 - \frac{x_n}{k}\right) - \beta(1 - e^{-a x_{n-\tau}})y_{n-\tau},$$

and

$$F_y(x_{n-\tau}, y_{n-\tau}, y_n) = \eta(1 - e^{-a x_{n-\tau}})y_{n-\tau} - \delta y_n.$$

To incorporate memory effects, we replace the forward difference operator

$$\Delta x_n = x_{n+1} - x_n, \qquad \Delta y_n = y_{n+1} - y_n,$$

by the Caputo-type discrete fractional difference operator ${}^C\Delta^\alpha$ (Definition 2.2). Consequently, the fractional deterministic system becomes

$$\begin{aligned} {}^C\Delta^\alpha x_{n+1} &= \mu F_x(x_n, x_{n-\tau}, y_{n-\tau}),\\ {}^C\Delta^\alpha y_{n+1} &= \mu F_y(x_{n-\tau}, y_{n-\tau}, y_n). \end{aligned} \tag{4.8}$$

Let $E^* = (x^*, y^*)$ denote a coexistence equilibrium of system (4.8). Define the perturbation variables

$$X_n = x_n - x^*, \qquad Y_n = y_n - y^*,$$

and

$$Z_n = \begin{pmatrix} X_n \\ Y_n \end{pmatrix}.$$

Linearizing the righthand side of (4.8) about the equilibrium E^*, we obtain the fractional linearized system

$$^{C}\Delta^{\alpha} Z_{n+1} = \mu \left(AZ_n + BZ_{n-\tau} \right), \tag{4.9}$$

where A and B are the Jacobian matrices associated with the current and delayed states, respectively.

Specifically,

$$A = \left. \frac{\partial (F_x, F_y)^T}{\partial (x_n, y_n)} \right|_{E^*}, \qquad B = \left. \frac{\partial (F_x, F_y)^T}{\partial (x_{n-\tau}, y_{n-\tau})} \right|_{E^*}.$$

The required partial derivatives are

$$\frac{\partial F_x}{\partial x_n} = r\left(1 - \frac{2x^*}{k}\right), \qquad \frac{\partial F_y}{\partial y_n} = -\delta,$$

$$\frac{\partial F_x}{\partial x_{n-\tau}} = -\beta a e^{-ax^*} y^*, \qquad \frac{\partial F_x}{\partial y_{n-\tau}} = -\beta(1 - e^{-ax^*}),$$

$$\frac{\partial F_y}{\partial x_{n-\tau}} = \eta a e^{-ax^*} y^*, \qquad \frac{\partial F_y}{\partial y_{n-\tau}} = \eta(1 - e^{-ax^*}).$$

Therefore,

$$A = \begin{pmatrix} r\left(1 - \dfrac{2x^*}{k}\right) & 0 \\ 0 & -\delta \end{pmatrix},$$

and

$$B = \begin{pmatrix} -\beta a e^{-ax^*} y^* & -\beta(1 - e^{-ax^*}) \\ \eta a e^{-ax^*} y^* & \eta(1 - e^{-ax^*}) \end{pmatrix}.$$

The stochastic perturbations are omitted in the derivation of the characteristic equation because they possess zero mean and therefore do not influence the deterministic stability boundary. Their effects are investigated separately through the mean-square stability analysis developed in the previous section. Such a separation between deterministic spectral analysis and stochastic stability analysis is standard in the theory of stochastic bifurcations and fractional dynamical systems (see [25, 26]).

Theorem 4.2 (Fractional characteristic equation)**.** *Consider the fractional linearized delayed system*

$$\Delta^{\alpha} Z_{n+1} = \mu(AZ_n + BZ_{n-\tau}),$$

where $A, B \in \mathbb{R}^{2\times 2}$ are the Jacobian matrices evaluated at the coexistence equilibrium E^*.
Then, the corresponding characteristic equation is

$$\det\left([(1 - \lambda^{-1})^{\alpha} I - \mu A]\lambda^{\tau} - \mu B \right) = 0. \tag{4.10}$$

Proof. Following the standard spectral approach for fractional difference equations [25, 26, 41], we seek a nontrivial solution of the form

$$Z_n = \lambda^n v, \qquad v \neq 0.$$

For the Grünwald–Letnikov fractional difference operator,

$$\Delta^\alpha \lambda^n = (1 - \lambda^{-1})^\alpha \lambda^n.$$

Substituting $Z_n = \lambda^n v$ into

$$\Delta^\alpha Z_{n+1} = \mu(AZ_n + BZ_{n-\tau})$$

gives

$$(1 - \lambda^{-1})^\alpha \lambda^n v = \mu\Big(A\lambda^n v + B\lambda^{n-\tau} v\Big).$$

Dividing by λ^n yields

$$\Big[(1 - \lambda^{-1})^\alpha I - \mu A - \mu\lambda^{-\tau} B\Big]v = 0.$$

Since $v \neq 0$, the coefficient matrix must be singular. Therefore,

$$\det\Big[(1 - \lambda^{-1})^\alpha I - \mu A - \mu\lambda^{-\tau} B\Big] = 0.$$

Multiplying by λ^τ gives (4.10).
The proof is complete.

□

Corollary 4.3 (Qualitative effect of fractional memory)**.** *Assume that the roots of the characteristic equation depend continuously on $\alpha \in (0, 1]$. Then decreasing α modifies the spectral distribution through the factor $(1 - \lambda^{-1})^\alpha$, which may increase the critical bifurcation threshold and delay the onset of oscillatory behavior. This observation is confirmed numerically in Section 5.*

Remark 4.1. *The deterministic part of the integer-order system* (3.2) *is written as a system of forward differences. Replacing the integer forward difference $\Delta x_n = x_{n+1} - x_n$ with the Caputo-type discrete fractional difference ${}^C\Delta^\alpha x_n$ (Definition 2.2) introduces memory effects. Linearizing this fractional deterministic system around the coexistence equilibrium (x^*, y^*) and omitting the zero-mean noise terms (which do not affect the bifurcation condition [36]) yields the linearized fractional equation.*

5. Numerical simulation and discussion

In Figure 2, the track for $\alpha = 0.85$ shows smooth rotation patterns, suggesting larger memory effects that delay the beginning of instability, slow oscillation decay, and stabilize the system. Alternatively, the trajectories become more inconsistent and scattered when $\alpha = 0.50$, suggesting reduced memory effects that produced early instability. Smaller fractional orders aggravate fluctuations and speed up oscillatory instabilities, while larger fractional orders generally give smoother dynamical transitions and delay bifurcations.

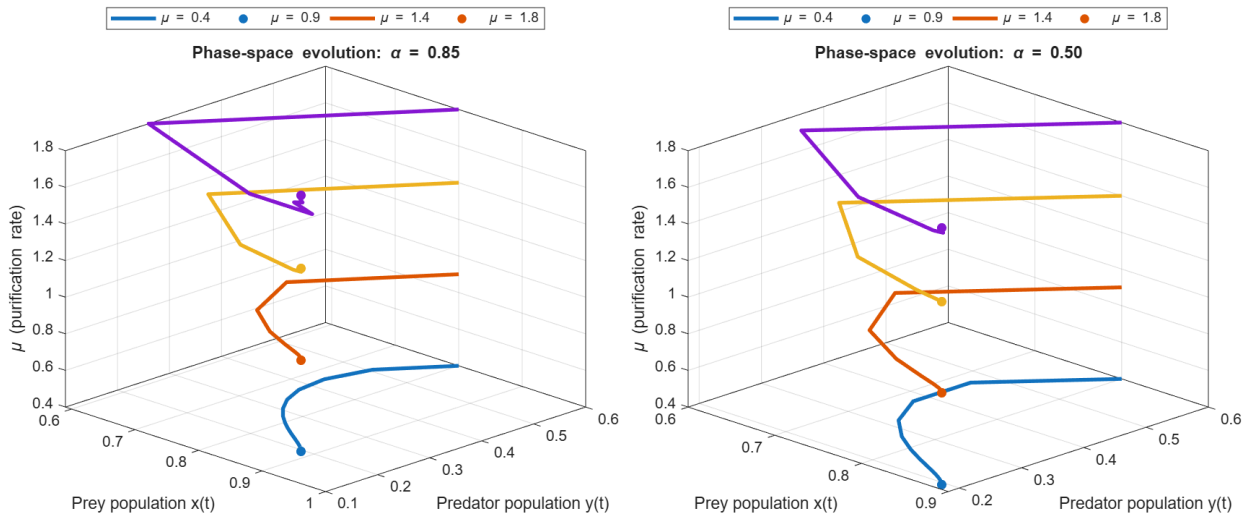

Figure 2. The fractional-delay model 3D phase-portrait shows the evolution of (x, y, μ) on two fractional orders. Left: $\alpha = 0.85$, bifurcation at $\mu_c \approx 1.15$; Right: $\alpha = 0.50$, delayed instability at $\mu_c \approx 1.35$.

In Figure 3, each set has equilibrium states as functions of μ, phase trajectories in the (x, y)-plane, and the controlling eigenvalue $|\lambda|$ vs the purification parameter μ. While smaller α produce a slower decay and broad trajectories, larger α increase memory effects and develop the faster convergence to coexistence and faster damping of oscillations. As μ grows, the stability curves demonstrate that $|\lambda|$ crosses the unit circle, indicating a Neimark-Sacker bifurcation. Alternatively, lower fractional orders show instability and more pronounced oscillatory behavior. Higher fractional orders delay this transition and preserve stability across a larger value of μ.

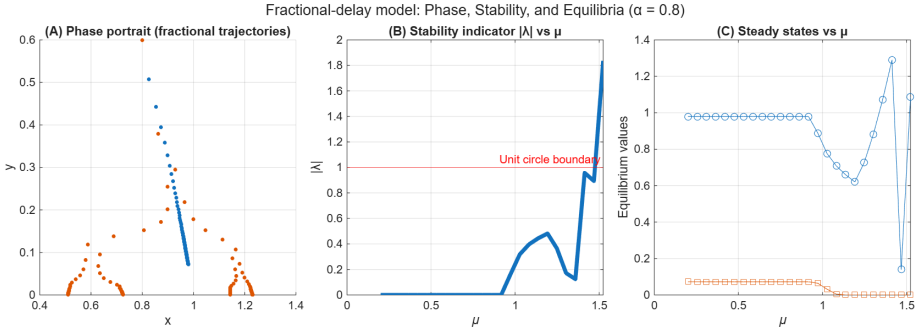

(a)

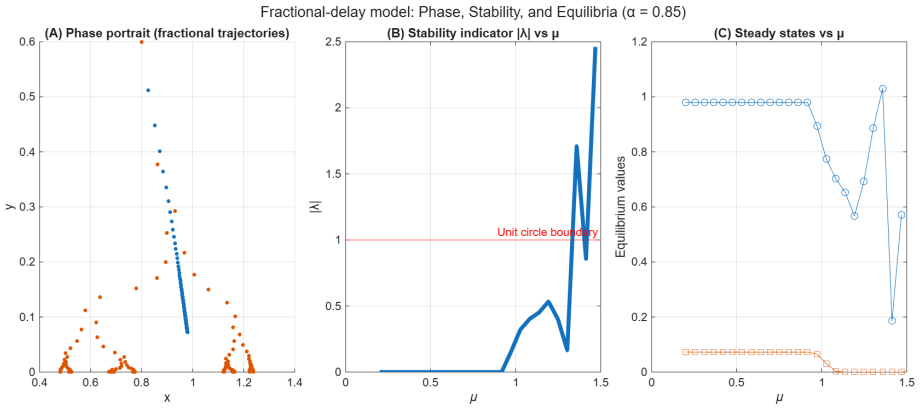

(b)

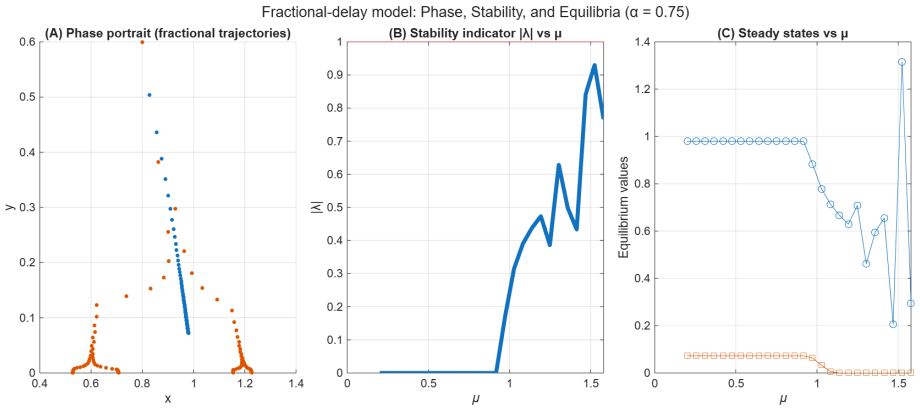

(c)

Figure 3. Phase portrait in (x, y) plane, equilibrium states vs μ, and maximum eigenvalue modulus vs μ for various fractional order.

Each subplot of Figure 4 produce trajectories in the (x, y) plane to show how increasing μ affects stability and convergence. Trajectories spiral fast toward the coexistence equilibrium with fast damped oscillations at lower levels $\mu = 0.40$ and 0.47, suggesting strong local stability. Convergence is still apparent at $\mu = 0.53$, but the transient oscillations are more pronounced, showing that a Neimark-Sacker bifurcation is forthcoming. Spirals are flatter and longer when μ rises to 0.60 and 0.67, indicating a weaker area of attraction and a slower decline. Near-marginal stability is shown by trajectories with nearly horizontal oscillations that approach the equilibrium relatively slowly for

$\mu = 0.80$. Overall, the subfigures show a progressive loss of stability as μ climbs toward the critical bifurcation threshold.

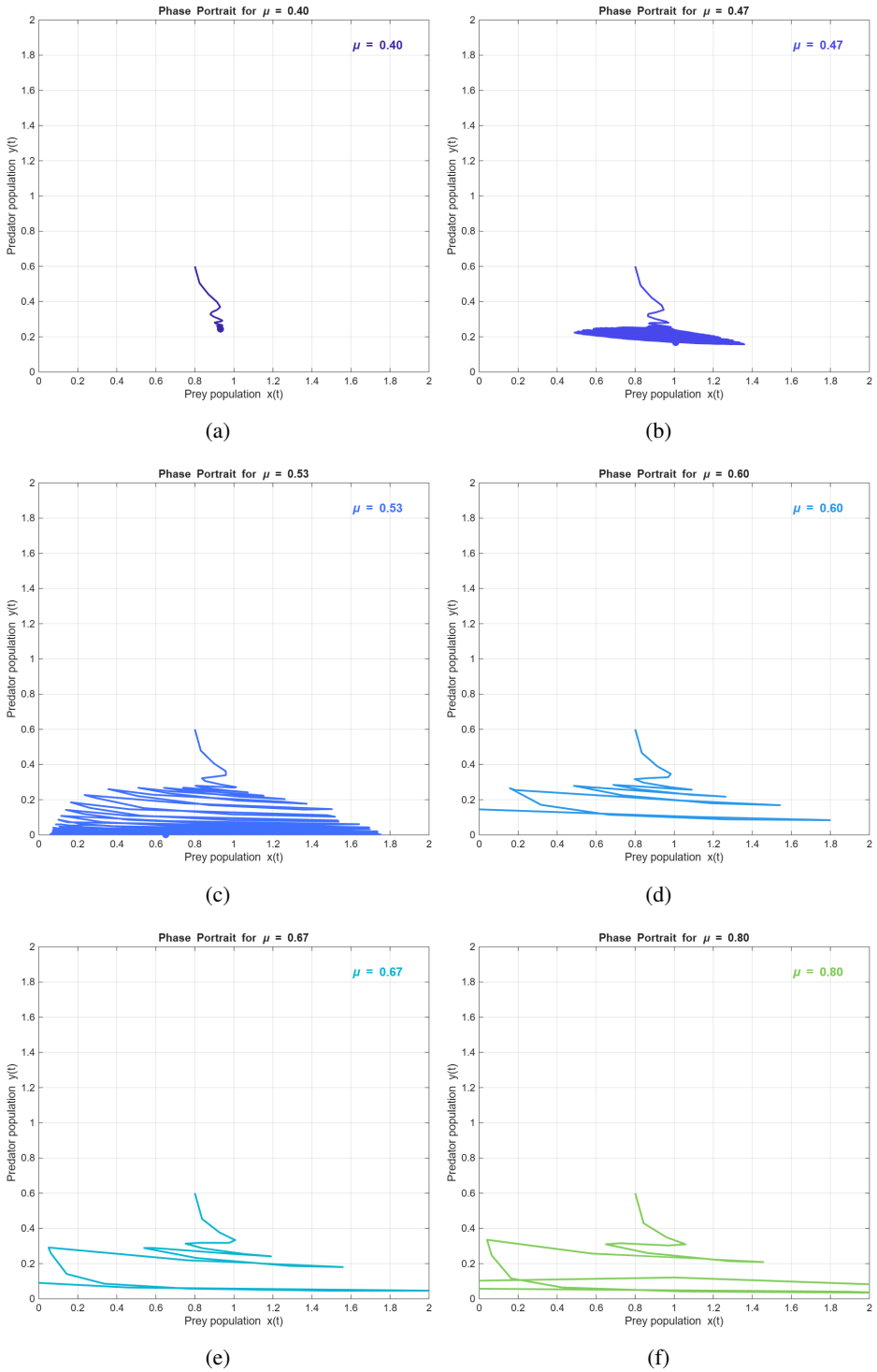

Figure 4. The fractional predator-prey model's phase portrait for different values of μ.

Figure 5 displays the time-series dynamics of the fractional stochastic delayed predator–prey model

for $\mu = 0.05$ and $\alpha = 0.95$ under three noise intensity pairs: $(\sigma_1, \sigma_2) = (0.04, 0.02)$, $(0.06, 0.04)$, and $(0.08, 0.06)$. The panels on the left and right, respectively, depict prey x_n and predator y_n. When both populations exhibit damped oscillations that converge to the coexistence equilibrium, mean-square stability is verified for low noise. As noise intensities increase, oscillations get bigger and continue longer, but convergence is still maintained even at the highest noise level. These results show the stabilizing function of strong fractional memory ($\alpha = 0.95$), which preserves long-term stability and lessens stochastic fluctuations, in accordance with the theoretical mean-square stability analysis.

The time evolution of the prey x_n and predator y_n populations for the fractional stochastic delayed predator–prey model with $\alpha = 0.90$ is shown in Figure 6. Both populations produce weak oscillations that decline to zero under moderate noise $(\sigma_1, \sigma_2) = (0.04, 0.02)$, displaying mean-square stability rising by fractional memory. During the trajectories becoming constrained and eventually converging to zero, temporary oscillations become larger and prevail longer when noise intensities increase to $(0.10, 0.08)$ and $(0.15, 0.14)$. The findings propose that integrating fractional memory with delay and nonlinear feedback helps to sustain stability, despite increasingly intense random disruptions.

Figure 7 investigates the time-series plots of prey and predator populations for $\alpha = 0.85$ and $\mu = 0.05$ subject to three noise intensity pairs. For low noise $(\sigma_1, \sigma_2) = (0.04, 0.02)$, both populations display fast damped oscillations that converge to the zero equilibrium, proving mean-square stability. When noise increases to $(0.06, 0.04)$ and $(0.10, 0.08)$, oscillations grow larger and last longer, although trajectories stay constrained and decline asymptotically. These findings demonstrate that fractional memory at $\alpha = 0.85$ effectively suppresses long-term stochastic fluctuations and preserves system stability in accordance with the theoretical mean-square stability criterion.

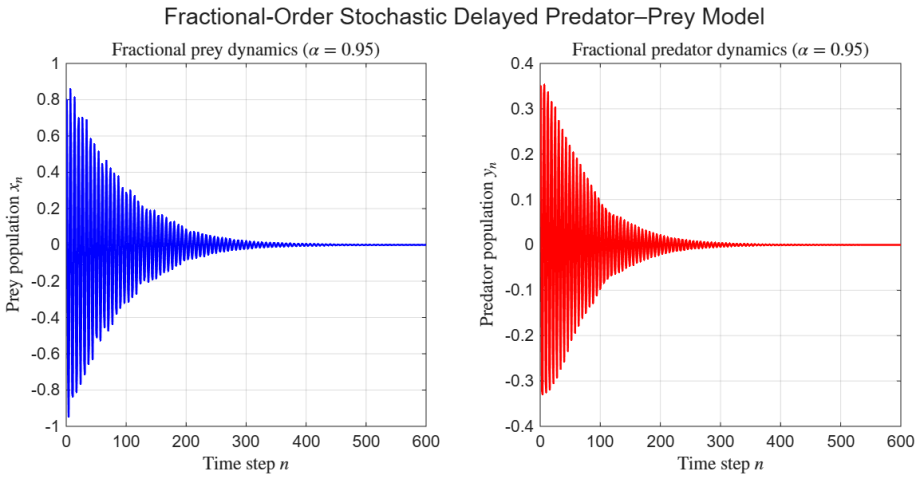

(a)

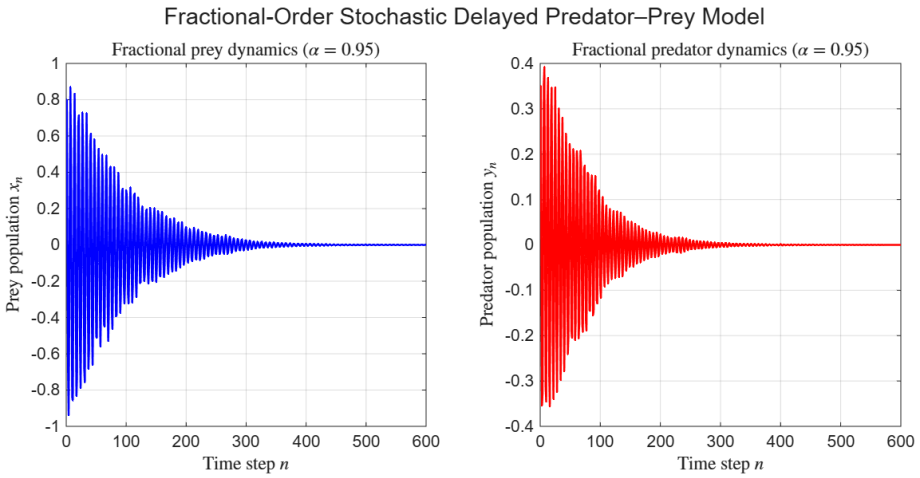

(b)

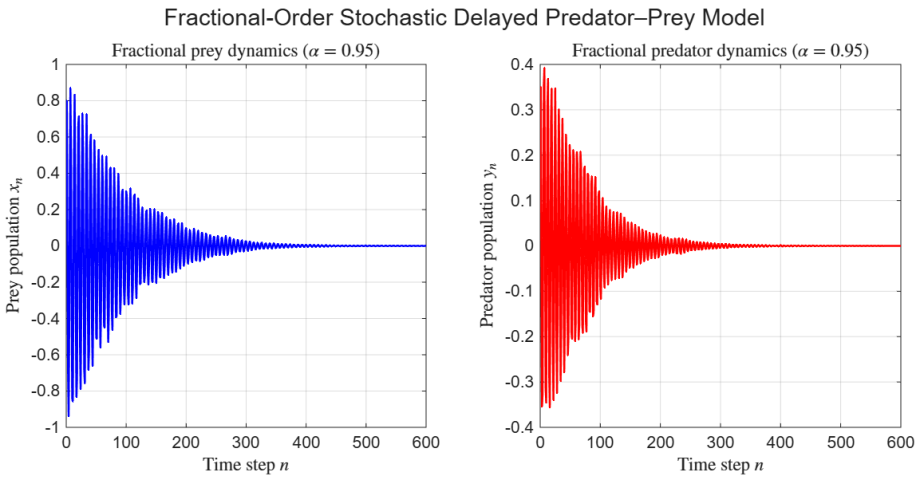

(c)

Figure 5. Time series of populations for the fractional-order stochastic delayed predator-prey model with $\mu = 0.05$ and fractional order $\alpha = 0.95$.

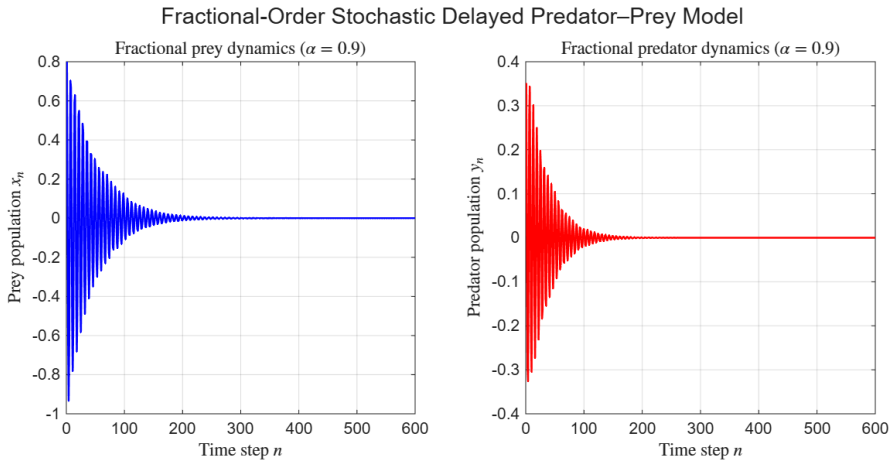

(a) $\sigma_1 = 0.04,\ \sigma_2 = 0.02$

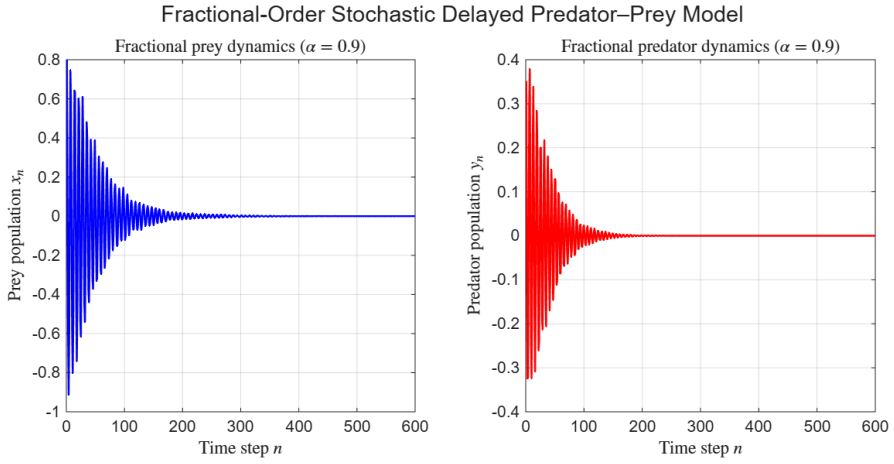

(b) $\sigma_1 = 0.10,\ \sigma_2 = 0.08$

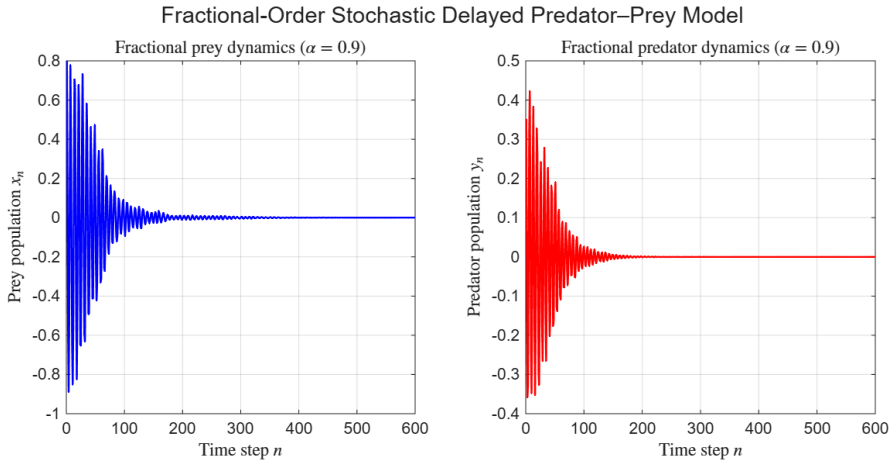

(c) $\sigma_1 = 0.15,\ \sigma_2 = 0.14$

Figure 6. Time series of prey population x_n and predator population y_n for the fractional-order stochastic delayed predator-prey model with $\mu = 0.05$ and fractional order $\alpha = 0.90$.

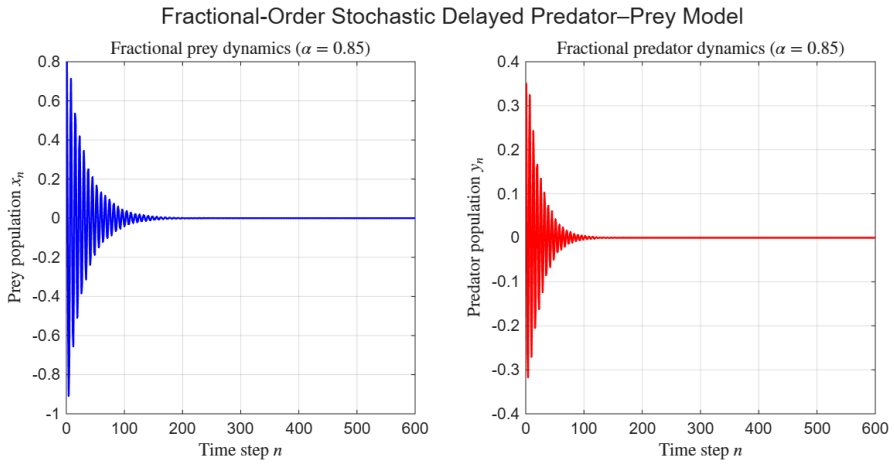

(a) $\sigma_1 = 0.04,\ \sigma_2 = 0.02$

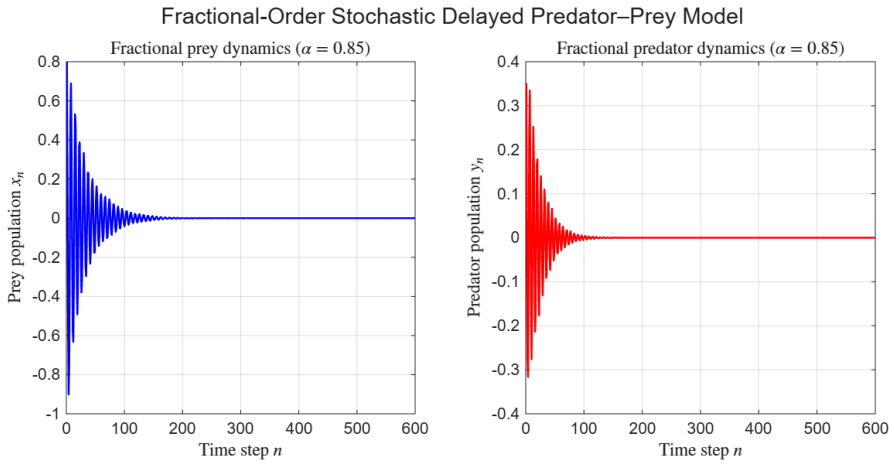

(b) $\sigma_1 = 0.06,\ \sigma_2 = 0.04$

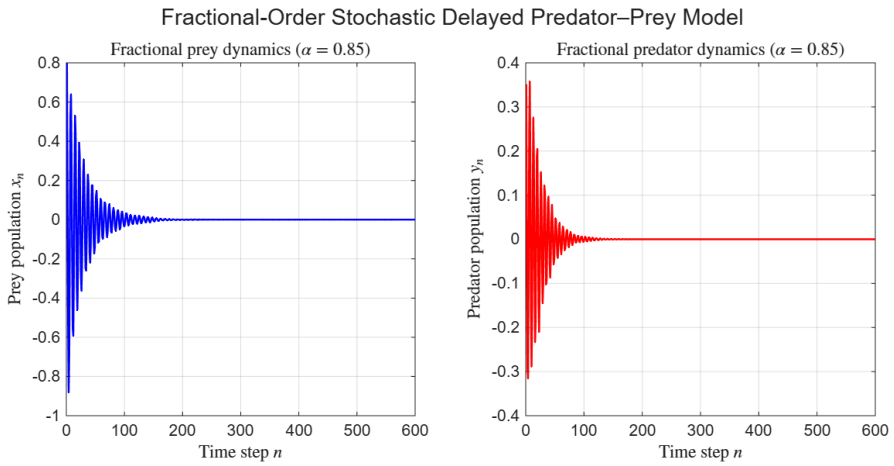

(c) $\sigma_1 = 0.15,\ \sigma_2 = 0.14$

Figure 7. Time series of prey population x_n and predator population y_n for the fractional-order stochastic delayed predator-prey model with $\mu = 0.05$ and fractional order $\alpha = 0.85$.

5.1. Numerical validation of theoretical results

In this section, we present numerical simulations to verify the analytical findings examined in the preceding sections. The simulations are used to verify the fractional-order stochastic delayed predator-prey model's boundedness, stability, bifurcation, and stochastic resilience properties, lemmas, and theorems.

5.1.1. Validation of positivity and boundedness results

When suitable parameter restrictions and a sufficiently small step size μ are used, lemmas related to positivity and uniform boundedness demonstrate that both prey and predator populations are nonnegative and bounded for any $n \geq 0$. The time-series simulations and phase pictures, which show that all numerical trajectories remain within biologically meaningful ranges without divergence or sign changes, corroborate this finding. In particular, the trajectories approach invariant absorbing sets, which is compatible with the explicit limitations found in Lemma 4.1 and the upper bounds of x_n and y_n in Propositions 4.2 and 4.1.

5.1.2. Validation of fractional-order memory effects

Nonlocal dampening effects are introduced by fractional-order memory, which supposedly stabilizes the system. This phenomenon is quantitatively confirmed by comparing time series and phase-space trajectories for different fractional orders. As the fractional order decreases from $\alpha = 0.95$ to $\alpha = 0.85$, the system exhibits a faster decline in oscillation amplitudes and better convergence to equilibrium. These results are consistent with memory-induced stability's analytical findings. 4.1 is the theorem.

5.1.3. Validation of mean square under stochastic perturbations

The stability Theorem 4.1 and the Corollary 4.1, which demonstrated first and second moment boundedness, established the mean-square stability prerequisites. The time series graphs for the predator and prey populations show that the solutions are still limited and converge asymptotically to equilibrium despite the short oscillations caused by random disturbances. The system does not show unbounded growth even at rising noise intensities, indicating that the mean square stability criteria are sufficient.

5.1.4. Combined effects of fractional memory and noise

Simulations for $\alpha = 0.95$ to $\alpha = 0.85$ are presented to illustrate the interplay between fractional memory and stochastic disturbances. The findings demonstrate that fractional memory extends the stability region by delaying instability and greatly reducing noise-induced oscillations. Our findings strongly confirm the theoretical Theorem 4.2, according to which fractional-order dynamics improve resistance to environmental unpredictability.

5.2. Numerical validation of the stability results

To complement the qualitative phase portraits and time-series simulations, we compute the spectral radius of the fractional characteristic equation at the coexistence equilibrium for different

fractional orders α. The equilibrium is locally asymptotically stable whenever the spectral radius satisfies $\rho(\alpha) < 1$. The convergence rate is measured by

$$R(\alpha) = -\ln(\rho(\alpha)),$$

where larger values of $R(\alpha)$ indicate faster convergence toward equilibrium.

Table 1 provides a quantitative assessment of the local stability of the coexistence equilibrium. For all considered fractional orders, the spectral radius satisfies $\rho(\alpha) < 1$, which confirms the local asymptotic stability predicted by the theoretical analysis. Moreover, the spectral radius increases monotonically as α increases from (0.75) to (1.00), while the corresponding convergence rate $R(\alpha) = -\ln(\rho(\alpha))$ decreases. This indicates that stronger memory effects (smaller α) are associated with faster convergence toward the equilibrium. These quantitative findings are consistent with the phase portraits and time-series simulations presented in Figures 1–6, where trajectories approach the equilibrium more rapidly for smaller values of α. Therefore, the spectral-radius analysis provides numerical support for the stability and memory-dependent behavior established in the theoretical results.

Table 1. Spectral radius of the fractional transition matrix and the corresponding convergence rate for the coexistence equilibrium under different fractional orders α.

Fractional order α	Spectral radius $\rho(\alpha)$	Convergence rate $R(\alpha)$
0.75	0.98519	0.014925
0.80	0.98735	0.012730
0.85	0.98923	0.010832
0.90	0.99085	0.009196
0.95	0.99224	0.007790
1.00	0.99344	0.006585

Remark 5.1. *In the numerical scheme, the fractional-memory contribution is first evaluated using the discrete fractional kernel, and the stochastic terms are then added locally. Thus, no interchange between the fractional and stochastic operators is required.*

Ecological implications of fractional memory. The fractional-order parameter α gives a mechanism for incorporating memory and hereditary impacts into predator-prey interactions. In contrast, in classical integer-order models, where population changes depend only on the current state, the fractional framework enables past ecological conditions to influence current dynamics. Such memory effects may arise from predator learning, adaptation to environmental variability, delayed reproductive responses, migration history, or accumulated resource availability. The numerical results indicate that smaller values of α produce stronger memory effects, leading to faster attenuation of oscillations and enhancing stability under stochastic disturbances. Ecologically, this suggests that populations possessing stronger historical dependence exhibit greater resilience against environmental fluctuations and are more robust to instability. Thus, fractional memory acts as a useful mechanism for describing realistic ecological processes and understanding long-term population persistence in fluctuating environments.

6. Conclusions and future work

This work developed and studied a unique discrete-time stochastic predator-prey model with time-delay and environment noise. The model accurately represented the complexity of real ecological systems by incorporating nonlinear predator-prey interactions, delay-induced feedback, and random perturbations. Analytical and numerical data were presented to illustrate the ways in which deterministic and stochastic elements interact to govern system stability and bifurcation events. The local stability requirements of the coexistence equilibrium have been determined using linearization techniques, and the Jury stability criterion and mean-square stability were analyzed. This study produced sufficient conditions that guarantee the asymptotic stability of the stochastic discrete system. Several claims and theorems were used to establish the stability boundaries and the mechanics of the change from oscillatory to stable regimes. A remarkable connection between numerical findings and theoretical outcomes was indicated by the analytical results, which were produced via MATLAB simulations and examples demonstrating how different dynamic behaviors, including oscillatory population cycles, quasi-periodic motion fluctuations, and stable coexistence, are led by the changes in system parameters, latency, and noise level. These results highlight how essential stochasticity and delay are to maintain the ecological equilibrium among species.

Author contributions

S. Khan and M. Darus: Supervision, writing–review and editing; S. Khan, M. Darus, J. Ro, and F. Tchier: Methodology, formal analysis, original draft. All authors read and approved the final manuscript.

Use of Generative-AI tools declaration

The authors declare they have not used Artificial Intelligence (AI) tools in the creation of this article.

Acknowledgments

First author work is supported by Ongoing Research Funding program, (ORF-2026-401), King Saudi University, Riyadh, Saudi Arabia.

Third author work was supported by the National Research Foundation of Korea(NRF) grant funded by the Korea government(MSIT)(RS-2026-25471383).

The fourth author was supported by Universiti Kebangsaan Malaysia.

Conflict of interest

The authors declare that they have no competing interests.

References

1. A. J. Lotka, *Elements of physical biology*, Williams & Wilkins, Baltimore, 1925.

2. V. Volterra, *Variazioni e fluttuazioni del numero d'individui in specie animali conviventi*, Società anonima tipografica "Leonardo da Vinci", 1926.
3. A. A. Berryman, The origins and evolution of predator–prey theory, *Ecology*, **73** (1992), 1530–1535. https://doi.org/10.2307/1940005
4. H. Singh, J. Dhar, H. S. Bhatti, Discrete-time bifurcation behavior of a prey–predator system with generalized predator, *Adv. Differ. Equations*, **2015** (2015), 206. https://doi.org/10.1186/s13662-015-0546-z
5. U. Ghosh, S. Sarkar, P. Chakraborty, Stability and bifurcation analysis of a discrete prey–predator model with mate-finding Allee effect, Holling type-I response and predator harvesting, *Braz. J. Phys.*, **52** (2022), 190. https://doi.org/10.1007/s13538-022-01189-2
6. V. S. Sharma, A. Singh, P. Malik, Bifurcation patterns in a discrete predator–prey model with ratio-dependent response and prey harvesting, *Qual. Theor. Dyn. Syst.*, **23** (2024), 74. https://doi.org/10.1007/s12346-023-00929-2
7. Y. A. Kuznetsov, H. G. Meijer, Numerical normal forms for codimension-2 bifurcations of fixed points with two critical eigenvalues, *SIAM J. Sci. Comput.*, **29** (2005), 1932–1954. https://doi.org/10.1137/030601508
8. Y. A. Kuznetsov, H. G. Meijer, *Numerical bifurcation analysis of maps*, Cambridge University Press, Cambridge, 2019.
9. C. S. Holling, The functional response of predators to prey density and its role in mimicry and regulation, *Memoirs Entomol. Soc. Canada*, **97** (1965), 5–60. https://doi.org/10.4039/entm9745fv
10. J. F. Andrews, A mathematical model for continuous culture of microorganisms using inhibitory substrates, *Biotechnol. Bioeng.*, **10** (1968), 707–723. https://doi.org/10.1002/bit.260100602
11. W. Sokol, J. A. Howell, Kinetics of phenol oxidation by washed cells, *Biotechnol. Bioeng.*, **23** (1981), 2039–2049. https://doi.org/10.1002/bit.260230909
12. V. S. Ivlev, Experimental ecology of the feeding of fishes, 1961.
13. K. S. Cheng, S. B. Hsu, S. S. Lin, Global stability results for a predator–prey system, *J. Math. Biol.*, **12** (1982), 115–126. https://doi.org/10.1007/BF00275207
14. R. E. Kooij, A. Zegeling, A predator–prey model with Ivlev's functional response, *J. Math. Anal. Appl.*, **198** (1996), 473–489. https://doi.org/10.1006/jmaa.1996.0093
15. P. A. Naik, R. Ahmed, A. Faizan, Bifurcation results for a Ricker-type discrete predator–prey system with a weak Allee effect, *Qual. Theor. Dynam. Syst.*, **23** (2024), 260.
16. I. G. Pearce, M. A. Chaplain, P. G. Schofield, A. R. Anderson, S. F. Hubbard, Spatiotemporal dynamics of multi-species host–parasitoid systems, *J. Theor. Biol.* **241** (2006), 876–886. https://doi.org/10.1016/j.jtbi.2006.01.026
17. K. F. Preedy, P. G. Schofield, M. A. Chaplain, S. F. Hubbard, Disease-induced dynamics in host–parasitoid systems: Chaos and coexistence, *J. Roy. Soc. Interface*, **4** (2007), 463–471. https://doi.org/10.1098/rsif.2006.0184
18. Z. Jing, J. Yang, Bifurcation and chaos in a discrete predator–prey system, *Chaos Soliton. Fract.*, **27** (2006), 259–277. https://doi.org/10.1016/j.chaos.2005.03.040

19. F. Courchamp, T. Clutton-Brock, B. Grenfell, Inverse density dependence and the Allee effect, *Trends Ecol. Evol.*, **14** (1999), 405–410. https://doi.org/10.1016/S0169-5347(99)01683-3

20. P. A. Stephens, W. J. Sutherland, Consequences of the Allee effect for behavioural ecology and conservation, *Trends Ecol. Evol.*, **14** (1999), 401–405. https://doi.org/10.1016/S0169-5347(99)01684-5

21. A. Ditta, P. A. Naik, R. Ahmed, Z. Huang, Periodicity and dynamical analysis in a harvested discrete commensalism system, *Int. J. Dynam. Control*, **13** (2025), 63.

22. M. A. McCarthy, The Allee effect, mate finding, and theoretical models, *Ecol. Model.*, **103** (1997), 99–102. https://doi.org/10.1016/S0304-3800(97)00104-X

23. B. Dennis, Allee effects: Population growth, critical density, and extinction risk, *Nat. Resour. Model.*, **3** (1989), 481–538. https://doi.org/10.1111/j.1939-7445.1989.tb00119.x

24. A. Kent, C. P. Doncaster, T. Sluckin, Predators under rescue and Allee effects on prey, *Ecol. Model.*, **162** (2003), 233–245. https://doi.org/10.1016/S0304-3800(02)00343-5

25. Y. Chatibi, E. H. El Kinani, A. Ouhadan, Variational calculus involving a nonlocal fractional derivative with a Mittag–Leffler kernel, *Chaos Soliton. Fract.*, **118** (2019), 117–121. https://doi.org/10.1016/j.chaos.2018.11.017

26. Y. Fan, X. Huang, Z. Wang, Y. Li, Nonlinear dynamics and chaotic behavior in a simplified memristor-based fractional-order neural network with discontinuous memductance, *Nonlinear Dynam.*, **93** (2018), 611–627. https://doi.org/10.1007/s11071-018-4213-2

27. K. M. Mutakabbir, U. M. Jasim, D. Fahim, S. Islam, R. S. M. Sohel, K. A. Qadeer, et al., Complex dynamics of a discrete prey–predator model on a complex network with stochasticity and a ratio-dependent Ivlev response, *Chaos*, **35** (2025), 033106. https://doi.org/10.1142/S0218127425400012

28. H. A. A. El-Saka, Backward bifurcations in fractional-order vaccination systems, *J. Egypt. Math. Soc.*, **23** (2015), 49–55. https://doi.org/10.1016/j.joems.2014.02.012

29. M. Javidi, N. Nyamoradi, Dynamic analysis of a fractional-order predator–prey interaction with harvesting, *Appl. Math. Model.*, **37** (2013), 8946–8956. https://doi.org/10.1016/j.apm.2013.04.024

30. Z. Cui, Z. Yang, Homotopy perturbation approach for fractional Lotka–Volterra models with variable coefficients, *J. Mod. Meth. Numer. Math.*, **5** (2014), 1–9. https://doi.org/10.20454/jmmnm.2014.767

31. P. A. Naik, Z. Eskandari, M. Yavuz, Z. Huang, Bifurcation and chaotic regimes in a discrete predator–prey model with a Holling-type predation response, *Discrete Cont. Dynam. Syst.-Ser. S*, **18** (2025), 1212–1229. https://doi.org/10.3934/dcdss.2024045

32. M. J. Uddin, C. N. Podder, Fractional-order predator–prey dynamics with prey immigration: Complexity and control, *Int. J. Biomath.*, **17** (2024), 2350051.

33. B. G. Pachpatte, *Inequalities for finite difference equations*, CRC Press, 2001.

34. S. Elaydi, *An introduction to difference equations*, 3 Eds., Springer, 2005.

35. M. R. S. Kulenović, G. Ladas, *Dynamics of second order rational difference equations*, Springer, 2002.

36. P. E. Kloeden, E. Platen, *Stochastic differential equations*, Springer Verlag, Berlin–Heidelberg, 1992.

37. X. Mao, *Stochastic differential equations and applications*, 2 Eds., Horwood Publishing, 2007.

38. D. J. Higham, Mean-square stability of numerical methods for stochastic differential equations, *SIAM J. Numer. Anal.*, **38** (2001), 753–769. https://doi.org/10.1137/S003614299834736X

39. Y. A. Kuznetsov, *Elements of applied bifurcation theory*, Springer Verlag, Berlin–Heidelberg, 2013.

40. P. A. Naik, Y. Javaid, R. Ahmed, Z. Eskandari, A. H. Ganie, Stability and bifurcation in a population model with an Allee effect via piecewise constant argument, *J. Appl. Math. Comput.*, **70** (2024), 4189–4218. https://doi.org/10.1007/s12190-024-02119-y

41. C. Goodrich, A. Peterson, *Discrete fractional calculus*, Springer, Cham, Switzerland, 2015.

AIMS Press